Available online at www.sciencedirect.com
SCIENCE DIRECT®
Journal of Crystal Growth 287 (2006) 189–193
JOURNAL OF CRYSTAL GROWTH
www.elsevier.com/locate/jcrysgro

# Structural and optical properties of ZnO nanosaws

Chun-Yi Wu[a], Hsu-Cheng Hsu[a], Hsin-Min Cheng[a,b], Song Yang[a], Wen-Feng Hsieh[a,*]

[a]*Department of Photonics & Institute of Electro-Optical Engineering, National Chiao Tung University, 1001 Tahsueh Rd., Hsinchu 30050, Taiwan*
[b]*Industrial Technology Research Institute, Hsinchu 310, Taiwan, ROC*

**Abstract**

The randomly oriented ZnO nanosaws were synthesized on Si substrates by a simple vapor transport method. For structure characterization of the products, the SEM micrograph clearly reveals that length of nanosaw exceeds several tens of μm and the side of sharp teeth of a saw has a length of about 1–5 μm and diameters of about 100 nm. The results of TEM, XRD, and Raman measurements indicate that the ZnO nanosaw is the single-crystal structure with the wurtzite phase. Under low excitation density, this UV emission peak measured at room temperature is attributed to the recombination of free excitons. Several sharp peaks emerge at photon energy around 3.18 eV with FWHM less than 4 meV when the sample is excited above a certain threshold. We refer that the random lasing in ZnO nanosaws results from the multiple coherent scattering in highly random-oriented ZnO nanosaws.


*PACS:* 42.55.Zz; 78.55.Et; 78.67.−n

*Keywords:* A1. Lasing; A1. Nanostructure; A1. Photoluminesence; B1. ZnO; B2. Semiconducting II–VI material

## 1. Introduction

During the past few years, research and development on the properties of all kinds of low-dimensional nanostructures have become important fundamental building blocks for nanophotonic devices and offer substantial promise for integrated nanosystems [1–3]. Much attention recently has been paid to the nano-structured materials such as ZnO and GaN, which radiate ultraviolet (UV) emission. Especially, ZnO has attracted considerable scientific and technological attention due to its wide direct band gap of 3.37 eV and large excitonic binding energy of 60 meV at room temperature. Therefore, ZnO nanostructures with different morphologies, such as nanowires and nanoribbon, have been fabricated for various potential applications, e.g., short-wavelength light-emitting diodes (LEDs) [4–5], room-temperature UV nanolaser [2,6], and solar cells [7–8]. Moreover, different morphologies of ZnO, such as nanowire, nanoneedle, nanocomb, nanoribbon, and nanocantilever have been fabricated and studied on their growth mechanisms [9–13].

In this article, we have successfully grown ZnO nanosaws by a simple vapor transport method and investigated their structural and optical properties. The transmission electron microscopy (TEM), X-ray diffraction (XRD), and Raman measurements indicate that the ZnO nanosaws possess single-crystal wurtzite structure and distribute randomly. Thus, the laser emission from ZnO nanosaws is believed to be random laser action due to coherent photon scattering as they were pumped beyond a threshold intensity [14]. It is found that the wavelength and the linewidth of the ZnO nanosaw random laser are at around 3.2 eV with FWHM less than 4 meV, respectively. This nontraditional way of light confinement has important applications to microlasers.

## 2. Experiments

Synthesis of ZnO nanosaws was achieved in a simple vapor transport process [15]. First, a very thin layer of Au was deposited on a (1 0 0)-silicon substrate. A mixture of

*Corresponding author. Tel.: +886 3 5712121x56316; fax: +886 3 5716631.
*E-mail address:* wfhsieh@mail.nctu.edu.tw (W.-F. Hsieh).

0022-0248/$ - see front matter © 2005 Elsevier B.V. All rights reserved.
doi:10.1016/j.jcrysgro.2005.10.065

pure zinc powder (99.9999%) and $Mg_3N_2$ powder (99.6%) with a weight ratio of 10:1 was placed in a ceramic boat as the starting materials. The boat was positioned in the center of the quartz furnace tube, and the substrate was placed 5 cm downstream from the mixed powder. After the high-purity argon gas had been infused into the system with a flow rate of 200 sccm, the furnace temperature was increased to 700 °C and kept at this temperature for 60 min under $O_2$ flow at about 2 sccm. After the reactions were complete, the system was cooled to the ambient temperature. Gray-white colored product was found deposited on the substrate.

The morphology, composition and crystallinity of the products were analyzed by scanning electron microscopy (SEM), energy-dispersive X-ray (EDX), TEM, and XRD. The optical characterization was studied by Raman and photoluminescence (PL) measurements. An Ar-ion laser of 5 mW with incident wavelength of 488 nm was used as the excitation source for the Raman spectroscopy. The scattered light was collected using backscattering geometry by the SPEX 1877 triplemate equipped with a liquid nitrogen cooled CCD. We used a He–Cd laser (325 nm) as the excitation source of cw PL measurement; and the third harmonic of Nd:$YVO_4$ laser (355 nm) with pulse width of ~500 ps and repetition rate of 1 kHz for pulsed pumping to study the laser emission. The emission light was dispersed by a TRIAX-320 spectrometer and detected by a UV-sensitive photomultiplier tube. All measurements were carried out at room temperature.

## 3. Results and discussion

As shown in Fig. 1(a), the typical SEM micrograph clearly reveals that a large quantity of the nanosaw was formed on the Si substrate. Typical length of nanosaws exceeds several tens of μm. The magnified SEM image is shown in the inset of Fig. 1(a). The saw-shaped nanostructure, with one side flat and the other side with teeth, is the most dominant morphology. The teeth of saw normally exceed length of about 1 μm with diameter ranging between 50 and 100 nm. The EDX spectrum shown in Fig. 1(b) reveals the nanosaws contain Zn and O elements without other detectable elements. Fig. 2(a) shows the TEM image of nanosaws. The width of the teeth is nearly 50 nm. The double image of the nanosaws is due to overlapping one on top of another. The selected-area electron diffraction (SAED) pattern is displayed in Fig. 2(b). The appearance of diffraction spot (0 0 0 2) confirms that teeth of a nanosaw growth along the *c*-axis direction. The discrete diffraction spots indicate that the ZnO nanosaw is hexagonal wurtzite single-crystalline as the previous reports [9–13].

Fig. 2(c) shows an HRTEM image taken from the side of teeth of a nanosaw, which indicates the perfect lattice structure of the nanosaw and the *d*-spacings between any two neighboring lattice fringes are 0.52 and 0.28 nm, which match (0 0 0 1) and (0 1 $\bar{1}$ 0) planes of the wurtzite ZnO, respectively. The growth mechanism of the nanosaws is

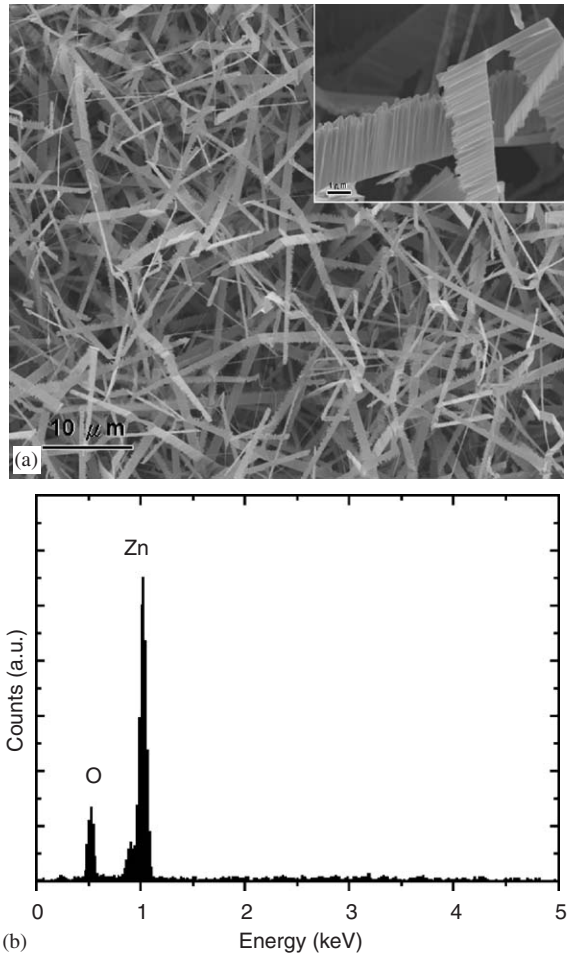


Fig. 1. (a) The SEM image of the ZnO nanosaws. The inset of (a) shows magnified SEM image of the ZnO nanosaws, and (b) the EDX of the ZnO nanosaws.

likely the self-catalyst process, which originates from Zn or $ZnO_x$ clusters. The possible growth procedure for typical ZnO nanosaw is as follow. The Zn powder turned into Zn vapor during the evaporation and formed Zn or $ZnO_x$ liquid droplets as the nucleation sites of the ZnO nanostructures, then the solid ZnO particles were condensed from the droplets. As the reaction process proceeded by repeating the above-mentioned processes, the condensed ZnO would continuously deposit on the nucleation sites to form the ZnO nanoribbons. Finally, it is known that [0 0 0 1] is the fastest growth direction along one side of ZnO nanostructures as reported in the comb-structures [11–13,15] that is responsible for the formation of ZnO nanosaws.

Fig. 3 shows the XRD pattern of the sample. All diffraction peaks and the corresponding relative intensities coincide with the JCPDS card no. 36-1451 to confirm the ZnO nanosaws possess the hexagonal wurtzite phase with the lattice constants: $a = 3.246$ and $c = 5.2$ Å. It is worth to notice that the relative intensities of all diffraction peaks of ZnO nanosaws are similar to those of ZnO powder. This implies that ZnO nanosaws are not only distributed but also oriented randomly on the Si substrate.

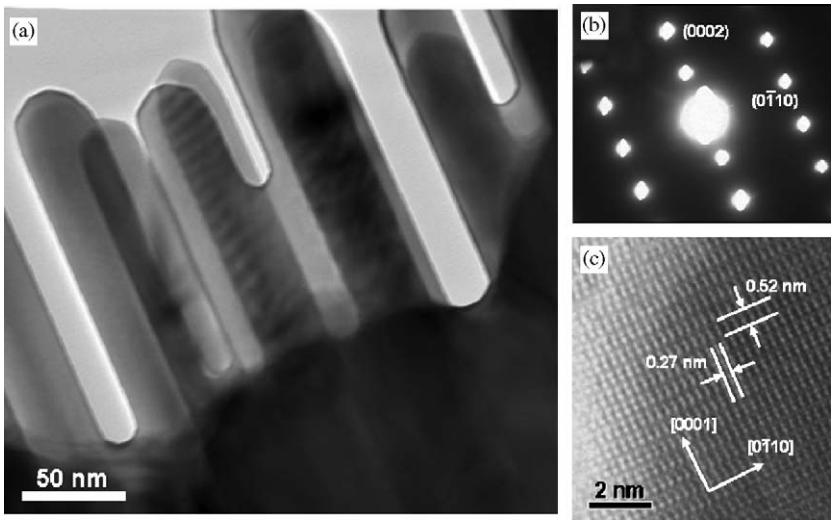


Fig. 2. (a)TEM image of the ZnO nanosaws, (b) SAED of the ZnO teeth and (c) HRTEM image of the teeth of the ZnO nanosaws.

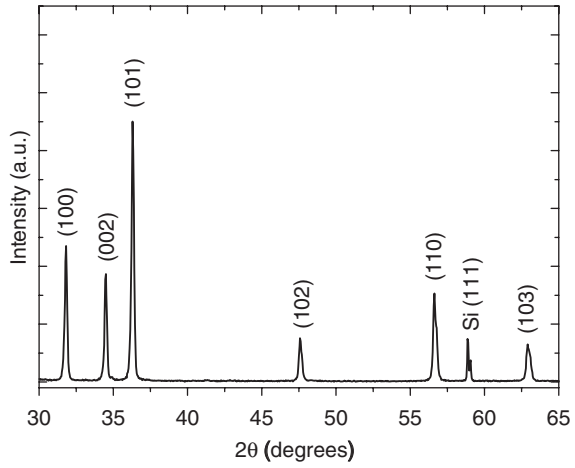


Fig. 3. The XRD pattern of the ZnO nanosaws.

The typical Raman spectrum of the ZnO nanosaws is shown in Fig. 4. The Raman peaks at 378 and 436 $cm^{-1}$ originate from vibration modes of A1(TO) (transverse optical, TO) and E2(high), respectively. The E2(high) mode corresponds to band characteristic of wurtzite phase. The Raman spectrum around 550–600 $cm^{-1}$ was attributed to the two polar symmetric longitudinal optical (LO) phonon modes, A1(LO) and E1(LO). Using A1(LO) and E1(LO) modes centered at 574 and 583 $cm^{-1}$, we found fitting quite well to the spectrum as the inset of Fig. 4. The result is consistent with that of ZnO powder (or bulk crystal) [16]. The appearance of the E1(LO) peak has been attributed to the formation of oxygen vacancy and interstitial zinc atom. [17]

The PL spectra of ZnO nanosaws measured at room temperature are shown in Fig. 5. Under cw laser excitation, the spectrum shows a strong UV emission peak having photon energy about 3.22 eV with FWHM ~150 meV and weak green band having a broad feature in the range of 1.9–2.8 eV. This sharp UV emission peak is attributed to the near band edge emission [18–19]. The emission of broad peak is the deep-level emission, which is attributed to the oxygen vacancy and Zn intersititial [20–21]. The strong UV emission and weak green emission in PL spectra indicate that the ZnO nanosaws have a good optical quality with few oxygen vacancies.

Fig. 6 shows dependence of emission spectra on the excitation intensity under pulse laser pumping. At low excitation intensity, the spectrum is composed of a single broad peak of spontaneous emission at 3.2 eV with FWHM ~115 meV which is similar to the cw PL spectrum. As increasing the excitation intensity, the emission becomes narrower due to the preferential amplification at wavelength close to the maximum of the gain spectrum. When the excitation intensity exceeded a threshold, $I_{th} = 0.96\,MW/cm^2$, several narrow peaks emerge in the emission spectra at around 3.18 eV, the line width of these peaks is less than 4 meV. When further increasing the pumping intensity, more sharp peaks appear and the intensity of the multiple sharp peaks increase much more rapidly with increasing pump intensity. These results indicate a clear evidence of lasing action. Note that the position of emission peak redshifts with increasing pumping intensity due to the band gap renormalization [22].

In general, the lasing action in ZnO nanostructures has two kinds of lasing mechanisms. The first type of lasing with the Fabry–Perot (FP) optical cavity arises from the structure of individual nanostructures, such as nanowire and nanoribbon [2,6]. The single-crystal nanostructure of ZnO is a gain medium by itself, which is provided by a natural optical cavity formed between the two-end facets and natural optical wave guide of the nanostructure. Another lasing mechanism is called ''random lasing''. The emitted light is strongly scattered in gain media and a close-loop path can be formed through multiple scattering. These loops could serve as ring cavity for light [14,22–23].

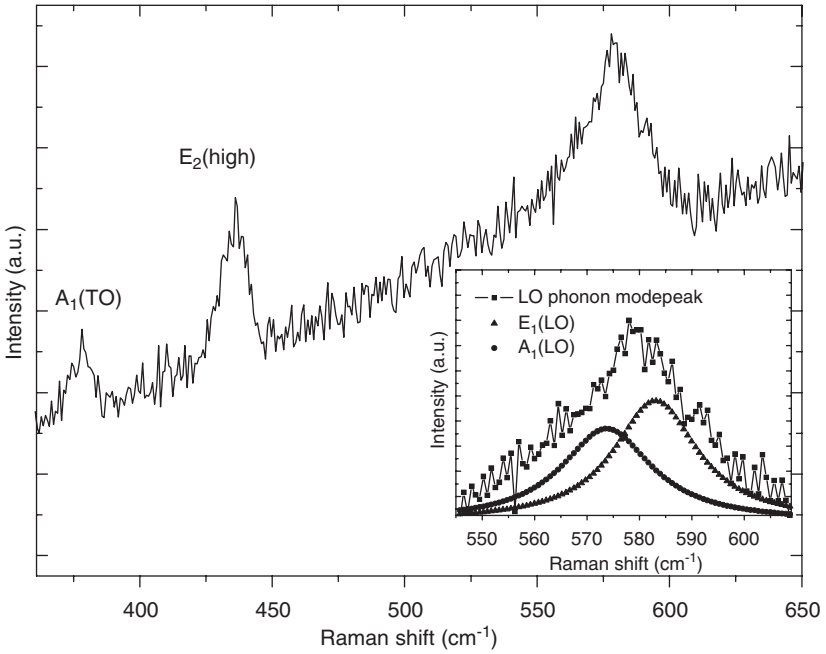


Fig. 4. The Raman spectra of the ZnO nanosaws.

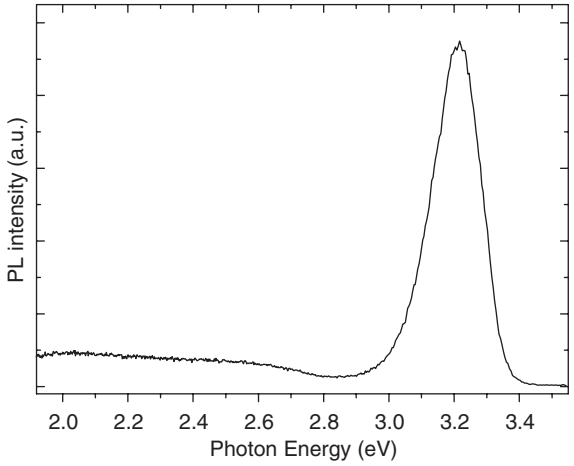


Fig. 5. The PL spectra of the ZnO nanosaws.

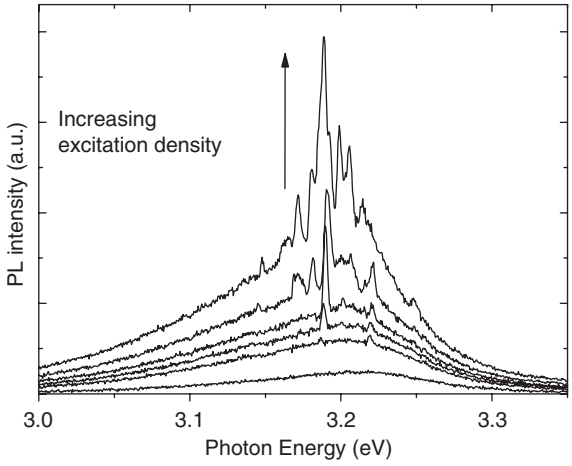


Fig. 6. The emission intensity of ZnO nanosaw versus the pumping intensity.

Based on the morphology of ZnO nanosaws (see Fig. 1) and the laser emission spectra in Fig. 6, we will further distinguish the two possible lasing behaviors as follows. From the longitudinal mode spacing ($\Delta\lambda$) of the lasing modes, we can determine the cavity length of a laser action by $\Delta\lambda = \lambda^2/(2nL)$, where $n$ is the refractive index of ZnO ($n = 2.45$) and $\lambda$ is the resonant wavelength $\sim$390 nm (photon energy = 3.18 eV). For a mode spacing between the closest longitudinal modes of about 0.65 nm, the cavity length is expected to be $\sim$50 μm. In spite of the ZnO nanosaw with length of about 50 μm might exist, the lasing action from FP mode is less likely to occur in ZnO nanosaws. Because the natural PF cavity formed in ZnO nanostructure needs both good crystalline and small internal loss [24]. The morphology of ZnO nanosaw is so rough that strong light scattering occurs at the interfaces of nanosaw. Moreover, the lasing emission peaks appear irregularly (see Fig. 6) as increasing the excitation intensity. It suggests that the lasing emission arises from different random cavities formed among the ZnO nanosaws. Therefore,it is much more possibly that the emitted light is scattered and feedback as a resonant cavity among the ZnO nanosaws.

To verify our laser cavities are "self-formed" by strong light scattering, we measured emission spectra at different excitation areas when the excitation intensity is fixed at 1.1 MW/cm$^2$. As shown in Fig. 7, before the excitation area reaches a threshold value, the scattered light has not yet gathered sufficiently in a certain close loop and thus no sharp peak emerges.When the excitation area has exceeded

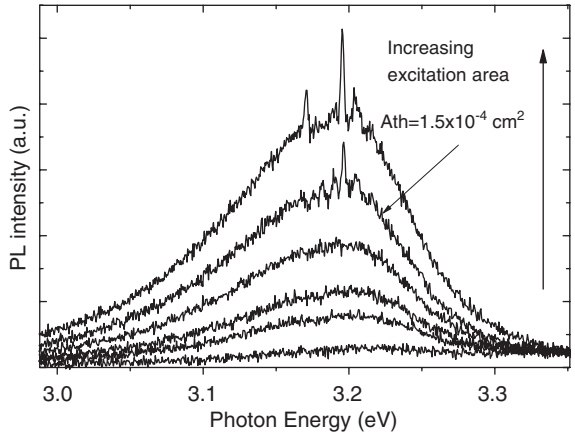


Fig. 7. The dependence of excitation area on emission spectra of the ZnO nanosaws.

the threshold area ($A_{th} = 1.5 \times 10^{-4}\,cm^2$), a closed path is formed through multiple scattering in the larger excitation area and the lasing action starts. Sharp peaks with line width of less than 5 meV were observed provided that laser cavities can be formed for suitable excitation area.

As a result of light scattering by the randomly distributed and oriented ZnO nanosaws, we can attribute the lasing behavior as random lasing among the ZnO nanosaws. Because of the short scattering mean free path, the emitted light is strongly scattered in ZnO nanosaws. Light is amplified while following a closed random path provided that it satisfies resonance condition due to coherent multiple scattering. These loops act as ring cavities, namely, the ring cavities are "self-formed" by reduplicating scattering.

## 4. Conclusion

In summary, ZnO nanostructures had been successfully grown by a vapor transport process. The results of TEM, XRD, and Raman measurements indicate that the ZnO nanostructure is the single-crystal structure with the wurtzite phase and confirms that teeth of the nanosaw growth along the *c*-axis direction. The growth mechanism of the nanosaws is suggested to be the self-catalyst process for the growth of oxide nanostructures without the existence of external metallic catalysts. The ZnO nanosaws exhibit strong UV emission and weak green emission, indicating very good optical quality. Under highly optical pumping, several sharp peaks emerge at about 3.18 eV with FWHM 4 meV. We have observed that random laser action without mirrors which is attributed to self-forming laser cavities via coherent multiple scattering in ZnO nanosaws.

## Acknowledgment

The authors would like to thank the National Science Council of the Republic of China under Contract No. NSC-93-2112-M-009-035.

## References

[1] X.F. Duan, Y. Huang, Y. Cui, J.F. Wang, C.M. Liber, Nature 409 (2001) 66.
[2] M. Huang, S. Mao, H. Feick, H. Yan, Y. Wu, H. Kind, E. Weber, R. Russo, P. Yang, Science 292 (2001) 1897.
[3] M. Law, D.J. Sirbuly, J.C. Johnson, J. Goldberger, R.J. Saykally, P. Yang, Science 305 (2004) 1269.
[4] A. Tsukazaki, A. Ohtomo, T. Onuma, M. Ohtani, T. Makino, M. Sumiya, K. Ohtani, S.F. Chichibu, S. Fuke, Y. Segawa, H. Ohno, H. Koinuma, M. Kawasaki, Nat. Mater. 4 (2005) 42.
[5] R. Könenkamp, R.C. Word, C. Schlegel, Appl. Phys. Lett. 85 (2004) 6004.
[6] H.Q. Yan, J. Johnson, M. Law, R.R. He, K. Knutsen, J.R. McKinney, J. Pham, R. Saykally, P.D. Yang, Adv. Mater. 15 (2003) 1907.
[7] J.B. Baxter, E.S. Aydil, Appl. Phys. Lett. 86 (2005) 053114.
[8] M. Law, L.E. Greene, J.C. Johnson, R. Saykally, P. Yang, Nat. Mater. 4 (2005) 455.
[9] M.H. Huang, Y. Wu, H. Feick, N. Tran, E. Weber, P. Yang, Adv. Mater. 13 (2001) 113.
[10] Y.K. Tseng, C.J. Huang, H.M. Cheng, I.N. Lin, K.S. Liu, I.C. Chen, Adv. Funct. Mater. 13 (2003) 811.
[11] C.X. Xu, X.W. Sun, Z.L. Dong, M.B. Yu, J. Crystal Growth 270 (2004) 498.
[12] Y.H. Leung, A.B. Djurišic, J. Gao, M.H. Xie, Z.F. Wei, S.J. Xu, W.K. Chan, Chem. Phys. Lett. 394 (2004) 452.
[13] Z.L. Wang, X.Y. Kong, J.M. Zuo, Phys. Rev. Lett. 91 (2003) 185502.
[14] H. Cao, J.Y. Xu, Y. Ling, A.L. Burin, E.W. Seeling, X. Liu, R.P.H. Chang, IEEE J. Sel. Top. Quantum Electron. 9 (2003) 111.
[15] H.C. Hsu, Y.K. Tseng, H.M. Chang, J.H. Kuo, W.F. Hsieh, J. Crystal Growth 261 (2004) 520.
[16] T.C. Damen, S.P.S. Porto, B. Tell, Phys. Rev. 142 (1966) 570.
[17] H.M. Cheng, H.C. Hsu, S.L. Chen, W.T. Wu, C.C. Kao, L.J. Lin, W.-F. Hsieh, J. Crystal Growth 277 (2005) 192.
[18] B.P. Zhang, N.T. Binh, Y. Segawa, Y. Kashiwaba, K. Haga, Appl. Phys. Lett. 84 (2004) 586.
[19] H.C. Hsu, W.-F. Hsieh, Solid State Commun. 131 (2004) 371.
[20] K. Vanheusden, W.L. Warren, C.H. Seager, D.R. Tallant, J.A. Voigt, B.E. Gnade, J. Appl. Phys. 95 (2004) 3141.
[21] X. Liu, W.H. Wu, H. Cao, R.P.H. Chang, J. Appl. Phys. 95 (2004) 3141.
[22] H.C. Hsu, C.Y. Wu, W.F. Hsieh, J. Appl. Phys. 97 (2005) 064315.
[23] S.F. Yu, C. Yuen, S.P. Lau, W.I. Park, G.C. Yi, Appl. Phys. Lett. 84 (2004) 3241.
[24] J.C. Johnson, H. Yan, P. Yang, R.J. Saykally, J. Phys. Chem. B 107 (2003) 8816.